

TOP QUARK MEASUREMENTS

A. JUSTE

Fermi National Accelerator Laboratory, P.O. Box 500, MS 357, Batavia, IL 60510, USA

E-mail: juste@fnal.gov

Ten years after its discovery at the Tevatron collider, we still know little about the top quark. Its large mass suggests it may play a key role in the mechanism of Electroweak Symmetry Breaking (EWSB), or open a window of sensitivity to new physics related to EWSB and preferentially coupled to it. To determine whether this is the case, precision measurements of top quark properties are necessary. The high statistics samples being collected by the Tevatron experiments during Run II start to incisively probe the top quark sector. This report summarizes the experimental status of the top quark, focusing in particular on the recent measurements from the Tevatron Run II.

1 Introduction

The top quark was discovered in 1995 by the CDF and DØ collaborations¹ during Run I of the Fermilab Tevatron collider. Like any discovery, this one caused a big excitement, although it did not really come as a surprise: the top quark existence was already required by self-consistency of the Standard Model (SM).

One of the most striking properties of the top quark is its large mass, comparable to the Electroweak Symmetry Breaking (EWSB) scale. Therefore, the top quark might be instrumental in helping resolve one of the most urgent problems in High Energy Physics: identifying the mechanism of EWSB and mass generation. In fact, the top quark may either play a key role in EWSB, or serve as a window to new physics related to EWSB and which, because of its large mass, might be preferentially coupled to it.

Ten years after its discovery, we still know little about the top quark. Existing indirect constraints on top quark properties from low-energy data, or the statistics-limited direct measurements at Tevatron Run I, are relatively poor and leave plenty of room for new physics. Precision measurements of top quark properties are crucial in order to unveil its true nature. Currently, the Tevatron collider is the world's only source of top quarks.

2 The Tevatron Accelerator

The Tevatron is a proton–antiproton collider operating at a center of mass energy of 1.96 TeV. With respect to Run I, the center of mass energy has been slightly increased (from 1.8 TeV) and the interbunch crossing reduced to 396 ns (from 3.6 μ s). The latter and many other upgrades to Fermilab's accelerator complex have been made with the goal of achieving a significant increase in luminosity. Since the beginning of Run II in March 2001, the Tevatron has delivered an integrated luminosity of $L = 1 \text{ fb}^{-1}$, and is currently operating at instantaneous luminosities $\mathcal{L} > 1 \times 10^{32} \text{ cm}^{-2}\text{s}^{-1}$. The goal is to reach $\mathcal{L} \sim 3 \times 10^{32} \text{ cm}^{-2}\text{s}^{-1}$ by 2007, and $L \sim 4.1 - 8.2 \text{ fb}^{-1}$ by the end of 2009. This represents a $\times 40 - 80$ increase with respect to the Run I data set, which will allow the Tevatron experiments to make the transition from the discovery phase to a phase of precision measurements of top quark properties.

3 Top Quark Production and Decay

At the Tevatron, the dominant production mechanism for top quarks is in pairs, mediated by the strong interaction, with a predicted cross section at $\sqrt{s} = 1.96 \text{ TeV}$ of $6.77 \pm 0.42 \text{ pb}$ for $m_t = 175 \text{ GeV}$.² Within the SM, top quarks can also be produced

singly via the electroweak interaction, with $\sim 40\%$ of the top quark pair production rate. However, single top quark production has not been discovered yet. While the production rate of top quarks at the Tevatron is relatively high, $\sim 2\,t\bar{t}$ events/hour at $\mathcal{L} = 1 \times 10^{32}\,\text{cm}^{-2}\text{s}^{-1}$, this signal must be filtered out from the approximately seven million inelastic proton-antiproton collisions per second. This stresses the importance of highly efficient and selective triggers.

Since $m_t > M_W$, the top quark in the SM almost always decays to an on-shell W boson and a b quark. The dominance of the $t \rightarrow Wb$ decay mode results from the fact that, assuming a 3-generation and unitary CKM matrix,³ $|V_{ts}|, |V_{td}| \ll |V_{tb}| \simeq 1$.⁴ The large mass of the top quark also results in a large decay width, $\Gamma_t \simeq 1.4\,\text{GeV}$ for $m_t = 175\,\text{GeV}$, which leads to a phenomenology radically different from that of lighter quarks. Because $\Gamma_t \gg \Lambda_{QCD}$, the top quark decays before top-flavored hadrons or $t\bar{t}$ -quarkonium bound-states have time to form.⁵ As a result, the top quark provides a unique laboratory, both experimentally and theoretically, to study the interactions of a bare quark, not masked by non-perturbative QCD effects.

Thus, the final state signature of top quark events is completely determined by the W boson decay modes: $B(W \rightarrow q\bar{q}') \simeq 67\%$ and $B(W \rightarrow \ell\nu_\ell) \simeq 11\%$ per lepton (ℓ) flavor, with $\ell = e, \mu, \tau$. In the case of $t\bar{t}$ decay, the three main channels considered experimentally are referred to as *dilepton*, *lepton plus jets* and *all-hadronic*, depending on whether both, only one or none of the W bosons decayed leptonically. The *dilepton* channel has the smallest branching ratio, $\sim 5\%$, and is characterized by two charged leptons (e or μ), large transverse missing energy (\cancel{E}_T) because of the two undetected neutrinos, and at least two jets (additional jets may result from initial or final state radiation). The *lepton plus jets* channel has a branching ratio of $\sim 30\%$ and is characterized by one charged lepton (e

or μ), large \cancel{E}_T and ≥ 4 jets. The largest branching ratio, $\sim 46\%$, corresponds to the *all-hadronic* channel, characterized by ≥ 6 jets. In all instances, two of the jets result from the hadronization of the b quarks and are referred to as b -jets. As it can be appreciated, the detection of top quark events requires a multipurpose detector with excellent lepton, jet and b identification capabilities, as well as hermetic calorimetry with good energy resolution.

4 The CDF and DØ detectors

The CDF and DØ detectors from Run I already satisfied many of the requirements for a successful top physics program. Nevertheless, they underwent significant upgrades in Run II in order to further improve acceptance and b identification capabilities, as well as to cope with the higher luminosities expected. CDF has retained its central calorimeter and part of the muon system, while it has replaced the central tracking system (drift chamber and silicon tracker). A new plug calorimeter and additional muon coverage extend lepton identification in the forward region. DØ has completely replaced the tracking system, installing a fiber tracker and silicon tracker, both immersed in a 2 T superconducting solenoid. DØ has also improved the muon system and installed new preshower detectors. Both CDF and DØ have upgraded their DAQ and trigger systems to accommodate the shorter interbunch time.

5 Top Quark Pair Production Cross Section

The precise measurement of the top quark pair production cross section is a key element of the top physics program. It provides a test of perturbative QCD and a sensitive probe for new physics effects affecting both top quark production and decay. Especially for the latter, the comparison of mea-

measurements in as many channels as possible is crucial. Also, by virtue of the detailed understanding required in terms of object identification and backgrounds, cross section analyses constitute the building blocks of any other top quark properties measurements. Finally, the precise knowledge of the top quark production cross section is an important input for searches for new physics having $t\bar{t}$ as a dominant background.

The measurements performed by CDF and DØ in Run I at $\sqrt{s} = 1.8$ TeV⁶ were found to be in good agreement with the SM prediction,⁷ but limited in precision as a result of the low available statistics ($(\Delta\sigma_{t\bar{t}}/\sigma_{t\bar{t}})_{stat} \sim 25\%$). In Run II, the large expected increase in statistics will yield measurements *a priori* only limited by systematic uncertainties. These include jet energy calibration, signal/background modeling, luminosity determination (currently $\sim 6\%$), etc. However, it is also expected that such large data samples will allow to control/reduce many of these systematic uncertainties. One example is the use of large dedicated control samples to constrain parameters (e.g. gluon radiation) in the modeling of signal and background processes. The goal in Run II is to achieve a per-experiment uncertainty of $\Delta\sigma_{t\bar{t}}/\sigma_{t\bar{t}} \leq 10\%$ for $L \simeq 2 \text{ fb}^{-1}$.

5.1 Dilepton Final States

Typical event selections require the presence of two high p_T isolated leptons (e, μ, τ or isolated track), large \cancel{E}_T and ≥ 2 high p_T central jets. Physics backgrounds to this channel include processes with real leptons and \cancel{E}_T in the final state such as $Z/\gamma^* \rightarrow \tau^+\tau^-$ ($\tau \rightarrow e, \mu$) and diboson production (WW, WZ, ZZ). The dominant instrumental backgrounds result from $Z/\gamma^* \rightarrow e^+e^-, \mu^+\mu^-$, with large \cancel{E}_T arising from detector resolution effects, and processes where one or more jets fake the isolated lepton signature ($W+jets$ or QCD multijets). Additional kinematic or topolog-

ical cuts are usually applied to further reduce backgrounds, such as e.g. on H_T (sum of p_T of jets in the event), exploiting the fact that jets from $t\bar{t}$ are energetic, whereas for backgrounds they typically arise from initial state radiation and have softer p_T spectra. CDF and DØ have developed different analysis techniques to exploit the potential of the sample. The *standard dilepton analysis* ($\ell\ell$), where two well identified leptons (e or μ) and at least two jets are required, has high purity ($S/B \geq 3$) but reduced statistics because of the stringent requirements on lepton identification and jet multiplicity. In order to improve the signal acceptance, the so-called *lepton+track analysis* ($\ell + track$) demands only one well identified lepton and an isolated track, and ≥ 2 jets (see Fig. 1). This analysis has increased acceptance for taus, in particular 1-prong hadronic decays. Finally, an *inclusive analysis* requiring two well identified leptons but placing no cuts on \cancel{E}_T or jet multiplicity, shows the potential for the greatest statistical sensitivity. In this analysis, a simultaneous determination of $\sigma_{t\bar{t}}$ and σ_{WW} is performed from a fit to the two-dimensional distribution of \cancel{E}_T vs jet multiplicity using templates from Monte Carlo (MC).

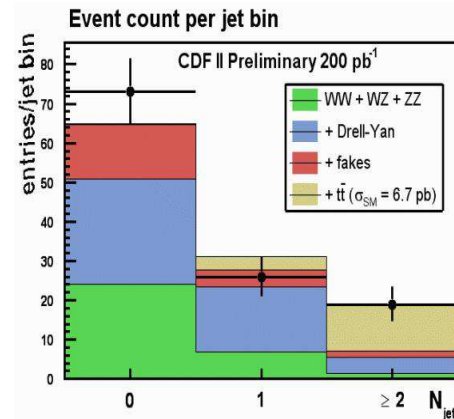


Figure 1. Jet multiplicity distribution for $t\bar{t}$ candidate events selected in the $\ell + track$ channel (CDF).

5.2 Lepton Plus Jets Final States

Typical event selections require one high p_T isolated lepton (e or μ), large \cancel{E}_T and ≥ 3 high p_T central jets. The dominant background is $W+jets$, followed by QCD multijets with one of the jets faking a lepton. After selection the signal constitutes $\sim 10\%$ of the sample. Further signal-to-background discrimination can be achieved by exploiting the fact that all $t\bar{t}$ events contain two b quarks in the final state whereas only a few percent of background events do. CDF and DØ have developed b -tagging techniques able to achieve high efficiency and background rejection: *lifetime tagging* and *soft-lepton tagging*. *Lifetime tagging* techniques rely upon B mesons being massive and long-lived, traveling ~ 3 mm before decaying with high track multiplicity. The high resolution vertex detector allows to directly reconstruct secondary vertices significantly displaced from the event primary vertex (secondary vertex tagging, or SVT) or identify displaced tracks with large impact parameter significance. *Soft-lepton tagging* is based on the identification within a jet of a soft electron or muon resulting from a semileptonic B decay. Only soft-muon tagging (SMT) has been used so far, although soft-electron tagging is under development and should soon become available. The performance of the current algorithms can be quantified by comparing the event tagging probability for $t\bar{t}$ and the dominant $W+jets$ background. For instance, for events with ≥ 4 jets: $P_{\geq 1-tag}(t\bar{t}) \simeq 60\%(16\%)$ whereas $P_{\geq 1-tag}(W+jets) \simeq 4\%$, using SVT(SMT). These analyses are typically pure counting experiments and are performed as a function of jet multiplicity in the event (see Fig. 2). Events with 3 or ≥ 4 jets are expected to be enriched in $t\bar{t}$ signal, whereas events with only 1 or 2 jets are expected to be dominated by background. The former are used to estimate $\sigma_{t\bar{t}}$, and the latter to verify the background normalization procedure.

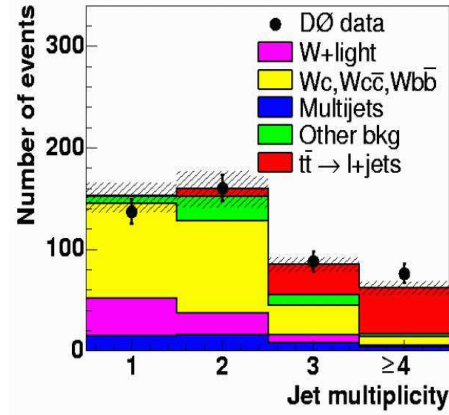


Figure 2. Jet multiplicity distribution for $t\bar{t}$ candidate events selected in the *lepton plus jets* channel, requiring at least one jet to be b -tagged by a secondary vertex algorithm (DØ).

cedure.

CDF and DØ have also developed analyses exploiting the kinematic and topological characteristics of $t\bar{t}$ events to discriminate against backgrounds: leptons and jets are more energetic and central and the events have a more spherical topology. The statistical sensitivity is maximized by combining several discriminant variables into a multivariate analysis (e.g. using neural networks), where the cross section is extracted from a fit to the discriminant distribution using templates from MC (see Fig. 3). Some of the dominant systematic uncertainties (e.g. jet energy calibration) can be reduced by making more inclusive selections (e.g. ≥ 3 jets instead of ≥ 4 jets). The combination of both approaches to improve statistical and systematic uncertainties have for the first time yielded measurements competitive with those using b -tagging (see Table 1).

5.3 All-Hadronic Final State

Despite its spectacular signature with ≥ 6 high p_T jets, the all-hadronic channel is extremely challenging because of the overwhelming QCD multijets background

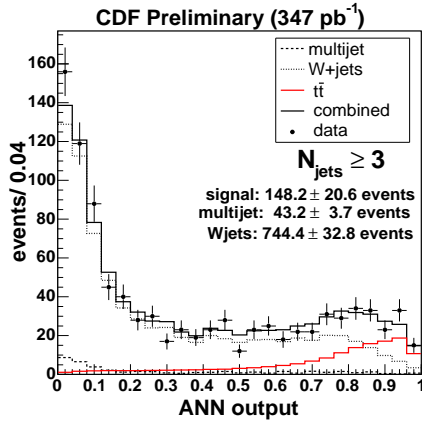


Figure 3. Neural network distribution for $t\bar{t}$ candidate events with ≥ 3 jets, selected in the *lepton plus jets* channel (CDF). This neural network exploits the kinematic and topological characteristics of $t\bar{t}$ events to discriminate against backgrounds.

($S/B \sim 1/2500$). Nevertheless, CDF and DØ successfully performed measurements of the production cross section and top quark mass in this channel in Run I. Current measurements by CDF and DØ focus on the b -tagged sample and make use of kinematic and topological information to further increase the signal-to-background ratio. CDF applies cuts on a set of four discriminant variables, whereas DØ builds an array of neural networks. In both cases, background is directly predicted from data.

5.4 Summary

Table 1 presents a summary of the best measurements in Run II in each of the different decay channels. Many more measurements have been produced by CDF and DØ and are available from their public webpages. So far, the different measurements are in agreement with each other and with the SM prediction. As precision continues to increase, the detailed comparison among channels will become sensitive to new physics effects. The single most precise measurement (*lepton plus jets*/SVT) has already

reached $\Delta\sigma_{t\bar{t}}/\sigma_{t\bar{t}} \sim 16\%$ and starts becoming systematics-limited. There is much work underway to further reduce systematic uncertainties as well as to combine the available measurements.

6 Top Quark Mass

The top quark mass (m_t) is a fundamental parameter of the SM, not predicted by the theory, and should be measured to the highest possible accuracy. In fact, it is an important ingredient in precision electroweak analyses, where some observables such as M_W receive loop corrections with a quadratic dependence on m_t . This fact was originally used to predict the value of m_t before the top quark discovery, which was ultimately found to be in good agreement with the experimental measurements and constituted a significant success of the SM. After the top quark discovery, the precise measurements of m_t and M_W can be used to constrain the value of the mass of the long-sought Higgs boson (M_H), since some of the electroweak precision observables also receive quantum corrections with a logarithmic dependence on M_H . The combined m_t from Run I measurements is $m_t = 178.0 \pm 4.3$ GeV,¹⁴ resulting on the preferred value of $M_H = 129_{-49}^{+74}$ GeV, or the upper limit $M_H < 285$ GeV at 95% C.L.. An uncertainty of $\Delta m_t \leq 2.0$ GeV would indirectly determine M_H to $\sim 30\%$ of its value.

Achieving such high precision is not an easy task, but the experience gained in Run I and the much improved detectors and novel ideas being developed in Run II provide a number of handles that seem to make this goal reachable. In Run I, the dominant systematic uncertainty on m_t was due to the jet energy scale calibration. The reason is that the top quark mass measurement requires a complicated correction procedure (accounting for detector, jet algorithm and physics effects) to provide a precise mapping between reconstructed jets and the original partons.

Table 1. Summary of the best $\sigma_{t\bar{t}}$ measurements at Tevatron Run II.

Channel	Method	$\sigma_{t\bar{t}}$ (pb)	L (pb $^{-1}$)	Experiment
Dilepton	$\ell\ell, \ell + track$	$7.0^{+2.4}_{-2.1}$ (stat.) $^{+1.7}_{-1.2}$ (syst.)	200	CDF ⁸
	$\ell\ell$	$8.6^{+3.2}_{-2.7}$ (stat.) ± 1.1 (syst.)	230	DØ ⁹
Lepton plus Jets	SVT	8.1 ± 0.9 (stat.) ± 0.9 (syst.)	318	CDF ¹⁰
	SVT	$8.6^{+1.2}_{-1.1}$ (stat.) $^{+1.1}_{-1.0}$ (syst.)	230	DØ ¹¹
	SMT	$5.2^{+2.9}_{-1.9}$ (stat.) $^{+1.3}_{-1.0}$ (syst.)	193	CDF ¹²
	Kinematic	6.3 ± 0.8 (stat.) ± 1.0 (syst.)	347	CDF
	Kinematic	$6.7^{+1.4}_{-1.3}$ (stat.) $^{+1.6}_{-1.1}$ (syst.)	230	DØ ¹³
All-Hadronic	SVT	7.8 ± 2.5 (stat.) $^{+4.7}_{-2.3}$ (syst.)	165	CDF
	SVT	$7.7^{+3.4}_{-3.3}$ (stat.) $^{+4.7}_{-3.8}$ (syst.)	162	DØ

To determine and/or validate the jet energy calibration procedure, data samples corresponding to *di-jet*, γ +jets and *Z+jets* production were extensively used. In addition to the above, the large $t\bar{t}$ samples in Run II allow for an *in situ* calibration of light jets making use of the W mass determination in $W \rightarrow jj$ from top quark decays, a measurement which is in principle expected to scale as $1/\sqrt{N}$. Also, dedicated triggers requiring displaced tracks will allow to directly observe $Z \rightarrow b\bar{b}$, which can be used to verify the energy calibration for b jets. Additional important requirements for the m_t measurement are: accurate detector modeling and state-of-the-art theoretical knowledge (gluon radiation, parton distribution functions, etc). The golden channel for a precise measurement is provided by the *lepton plus jets* final state, by virtue of its large branching ratio and moderate backgrounds, as well as the presence of only one neutrino, which leads to over-constrained kinematics. Powerful b -tagging algorithms are being used to reduce both physics and combinatorial backgrounds, and sophisticated mass extraction techniques are being developed, resulting in improvements in statistical as well as systematic uncertainties. An overview of the main analysis methods is given next.

6.1 Template Methods

These methods, traditionally used in Run I, start by constructing an event-by-event variable sensitive to m_t , e.g. the reconstructed top quark mass from a constrained kinematic fit in the *lepton plus jets* channel. The top quark mass is extracted by comparing data to templates on that particular variable built from MC for different values on m_t . Recent developments in this approach by CDF (see Fig. 4) have lead to the single most precise measurement to date: $m_t = 173.5^{+3.7}_{-3.6}$ (stat. + JES) ± 1.7 (syst.) GeV, exceeding in precision the current world average. The statistical uncertainty is minimized by separately performing the analysis in four subsamples with different b -tag multiplicity, thus each with a different background content and sensitivity to m_t . The dominant systematic uncertainty, jet energy calibration (JES), is reduced by using the *in situ* W mass determination from $W \rightarrow jj$ in a simultaneous fit of m_t and a jet energy calibration factor. The latter is also subjected to a constraint of $\sim 3\%$ from an external measurement in control samples. The remaining systematic uncertainties, amounting to $\Delta m_t = 1.7$ GeV, include contributions such as background shape, b -fragmentation, gluon radiation, parton distribution functions, etc,

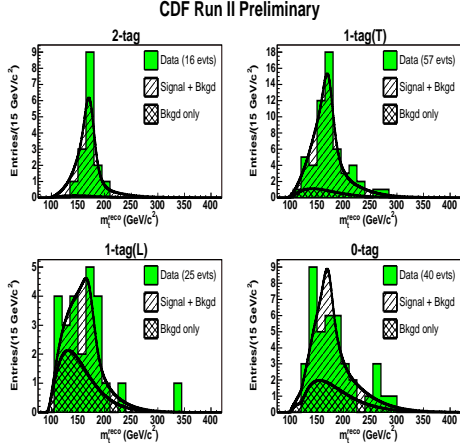


Figure 4. Reconstructed m_t distribution from a constrained kinematical fit in the *lepton plus jets* channel (CDF). The distribution is shown separately for the different subsamples defined based on the b -tag multiplicity.

many of which are expected to be further reduced with larger data samples.

6.2 Dynamic Methods

The main objective of these methods is to make an optimal use of the statistical information of the sample. They are based on the calculation of the per-event probability density as function of m_t , taking into account resolution effects (better measured events contribute more) and summing over all permutations of jets as well as neutrino solutions. These methods typically include a complete or partial matrix element evaluation for the signal and dominant background processes. The so-called *Matrix Element Method* was pioneered by DØ and applied to the *lepton plus jets* Run I sample¹⁵, leading to the single most precise measurement in Run I. In Run II, CDF has applied this method to the b -tagged *lepton plus jets* sample yielding a result competitive with the template method discussed above, and to the *lepton+track* sample, achieving the unprecedented accuracy in the *dilepton* channel of $m_t = 165.3 \pm 7.2$ (stat. + syst.) GeV.

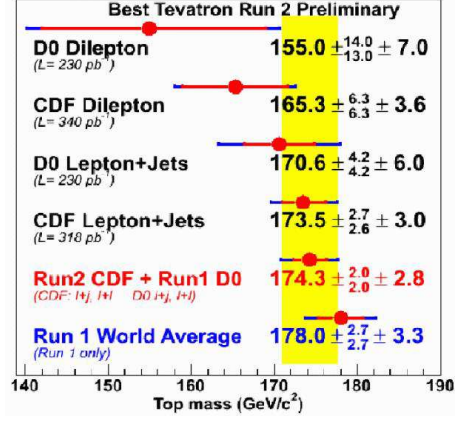


Figure 5. Summary of the best m_t measurements at Tevatron Run II.

6.3 Summary and Prospects

Fig. 5 summarizes the best Run II measurements for CDF and DØ in the different analysis channels. As it can be appreciated, some of the Run II individual measurements are already achieving uncertainties comparable or better than the Run I world average. The new preliminary combination of the DØ Run I and CDF Run II measurements in the *lepton plus jets* and *dilepton* channels yields: $m_t = 174.3 \pm 3.4$ GeV, $\chi^2/dof = 3.6/3$, improving upon the previous world average result. The resulting constraints on the Higgs boson mass are: $M_H = 98^{+52}_{-36}$ GeV or $M_H < 208$ GeV at 95% C.L.. Based on the current experience with Run II measurements, it is expected that an uncertainty of $\Delta m_t \leq 1.5$ GeV can be achieved at the Tevatron with 2 fb⁻¹, a precision which will probably be only matched by the LHC and will have to wait for the ILC to be exceeded.

7 Top Quark Couplings to the W boson

If the top quark is indeed playing a special role in the EWSB mechanism, it may have non-SM interactions to the weak gauge bosons. At the Tevatron, only the tWb ver-

tex can be sensitively probed. The LHC will have in addition sensitivity to certain ttZ couplings.¹⁶

Within the SM, the charge current interactions of the top quark are of the type V–A and completely dominated by the tWb vertex by virtue of the fact that $|V_{tb}| \simeq 1$. In fact, the tWb vertex defines most of the top quark phenomenology: it determines the rate of single top quark production and completely saturates the top quark decay rate. It is also responsible for the large top quark width, that makes it decay before hadronizing, thus efficiently transmitting its spin to the final state. The angular distributions of the top quark decay products also depend on the structure of the tWb vertex.

7.1 Single Top Quark Production

Within the SM, the main production mechanisms for single top quarks at the Tevatron involve the exchange of a timelike W boson (s-channel), $\sigma_s = 0.88 \pm 0.07$ pb, or a space-like W boson (t-channel), $\sigma_t = 1.98 \pm 0.21$ pb.¹⁷ Despite the relatively large expected rate, single top production has not been discovered yet. Upper limits on the production cross sections were obtained in Run I: $\sigma_s < 18$ pb, $\sigma_t < 13$ pb, $\sigma_{s+t} < 14$ pb (CDF) and $\sigma_s < 17$ pb, $\sigma_t < 22$ pb (DØ) at 95% C.L.. The experimental signature is almost identical to the *lepton plus jets* channel in $t\bar{t}$: high p_T isolated lepton, large \cancel{E}_T and jets, but with lower jet multiplicity (typically 2 jets) in the final state, which dramatically increases the W +jets background. In addition, $t\bar{t}$ production becomes a significant background with a very similar topology (e.g. if one lepton in the *dilepton* channel is not reconstructed).

Once it is discovered, the precise determination of the single top production cross section will probe, not only the Lorentz structure, but also the magnitude of the tWb vertex, thus providing the only direct measure-

ment of $|V_{tb}|$. The sensitivity to anomalous top quark interactions is enhanced by virtue of the fact that top quarks are produced with a high degree of polarization. In addition, the s- and t-channels are differently sensitive to new physics effects,¹⁸ so the independent measurement of σ_s and σ_t would allow to discriminate among new physics models should any deviations from the SM be observed.

In Run II the search for single top quark production continues with ever increasing data samples, improved detector performance, and increasingly more sophisticated analyses. The generic analysis starts by selecting *b*-tagged *lepton plus ≥ 2 jets* candidate events. CDF considers one discriminant variable per channel (e.g. $Q(\ell) \times \eta(\text{untagged jet})$ for the t-channel search) whereas DØ performs a multivariate analysis using neural networks (see Fig. 6). The upper limit on σ is estimated exploiting the shape of the discriminant variable and using a Bayesian approach. From ~ 162 pb⁻¹ data, CDF obtains the following observed (expected) 95% C.L. upper limits:¹⁹ $\sigma_s < 13.6(12.1)$ pb, $\sigma_s < 10.1(11.2)$ pb and $\sigma_{s+t} < 17.8(13.6)$ pb. The world's best limits are obtained by DØ from ~ 230 pb⁻¹ of data as a result of their more sophisticated analysis:²⁰ $\sigma_s < 6.4(5.8)$ pb and $\sigma_s < 5.0(4.5)$ pb. Both collaborations continue to add more data and improve their analyses and more sensitive results are expected soon.

7.2 W boson helicity in Top Quark Decays

While only single top quark production gives direct access to the magnitude of the tWb interaction, $t\bar{t}$ production can still be used to study its Lorentz structure. This is possible because the W boson polarization in top quark decays depends sensitively on the tWb vertex. Within the SM (V–A interaction), only two W boson helicity configurations, $\lambda_W = 0, -1$, are allowed. The frac-

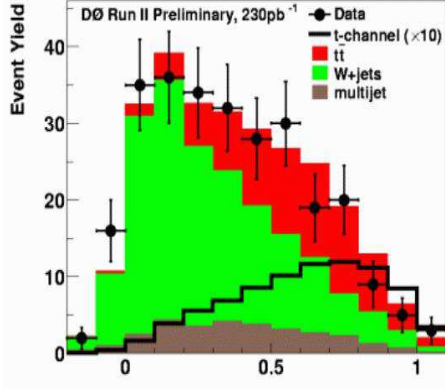


Figure 6. Neural network distribution for single top quark candidate events in the b -tagged $lepton\ plus\ \geq 2\ jets$ sample (DØ). This neural network has been optimized to discriminate between tb (s -channel) and $Wb\bar{b}$.

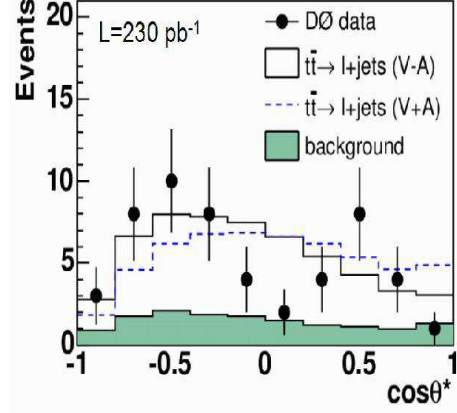


Figure 7. Lepton helicity angle distribution in the b -tagged $lepton\ plus\ \geq 4\ jets$ sample (DØ).

tion of longitudinal ($\lambda_W = 0$) and left-handed ($\lambda_W = -1$) W bosons are completely determined by the values of m_t , M_W and m_b and predicted to be: $F_0 \simeq 70\%$ and $F_- \simeq 30\%$, respectively (as a result, $F_+ \simeq 0\%$). The well-known quiral structure of the W interaction to leptons allows to use lepton kinematic distributions such as the p_T in the laboratory frame ($p_{T\ell}$) or the cosinus of the lepton decay angle in the W boson rest frame with respect to the W direction ($\cos\theta_\ell^*$) to measure the W helicity fractions. The $p_{T\ell}$ method can be applied to both $lepton\ plus\ jets$ and $dilepton$ final states. The $\cos\theta_\ell^*$ method can only be used in the $lepton\ plus\ jets$ final state since explicit top quark reconstruction is required.

Current Run II measurements by CDF and DØ are based on $\sim 200 - 230\text{ pb}^{-1}$ of data and, due to the still limited statistics, only consider the measurement of one W helicity fraction at a time, fixing the other one to the SM prediction. From the $p_{T\ell}$ method and using an unbinned likelihood, CDF has measured $F_0 = 0.27^{+0.35}_{-0.21}$ (stat. + syst.). DØ has instead focused on the $\cos\theta_\ell^*$ method to measure F_+ (see Fig. 7), using a binned likelihood.²¹ The result from the combination of two analyses (b -tag and kinematic)

is $F_+ < 0.25$ at 95% C.L.. The best measurements in Run I yielded²² $F_0 = 0.56 \pm 0.31$ (stat. + syst.) (DØ) and $F_+ < 0.18$ at 95% C.L. (CDF). All measurements, although still limited by statistics, are consistent with the SM prediction. The large expected samples in Run II should allow to make more sensitive measurements in the near future.

7.3 $B(t \rightarrow Wb)/B(t \rightarrow Wq)$

Assuming a 3-generation and unitary CKM matrix, $B(t \rightarrow Wb) = \Gamma(t \rightarrow Wb)/\Gamma_t \simeq 1$. An observation of $B(t \rightarrow Wb)$ significantly deviating from unity would be a clear indication of new physics such as e.g. a fourth fermion generation or a non-SM top quark decay mode. $\Gamma(t \rightarrow Wb)$ can be directly probed in single top quark production, via the cross section measurement. Top quark decays give access to $R \equiv B(t \rightarrow Wb)/B(t \rightarrow Wq)$, with $q = d, s, b$, which can be expressed as $R = \frac{|V_{tb}|^2}{|V_{td}|^2 + |V_{ts}|^2 + |V_{tb}|^2}$, and it's also predicted in the SM to be $R \simeq 1$.

R can be measured by comparing the number of $t\bar{t}$ candidates with 0, 1 and 2 b -tagged jets, since the tagging efficiencies for jets originating from light (d, s) and b quarks are very different. In Run I, CDF

measured²³ $R = 0.94^{+0.31}_{-0.24}$ (stat. + syst.). In Run II, both CDF and DØ have performed this measurement using data samples of $\sim 160 \text{ pb}^{-1}$ and $\sim 230 \text{ pb}^{-1}$, respectively. CDF considers events in both the *lepton plus jets* and *dilepton* channels and measures²⁴ $R = 1.12^{+0.27}_{-0.23}$ (stat. + syst.), whereas DØ only considers events in the *lepton plus jets* channel and measures $R = 1.03^{+0.19}_{-0.17}$ (stat. + syst.). All measurements are consistent with the SM prediction.

8 FCNC Couplings of the Top Quark

Within the SM, neutral current interactions are flavor-diagonal at tree level. Flavor Changing Neutral Current (FCNC) effects are loop-induced and thus heavily suppressed (e.g. $B(t \rightarrow c\gamma) \simeq 10^{-10}$, $B(t \rightarrow c\gamma/Z) \simeq 10^{-12}$), so an observation would be a clear signal of new physics. Indeed, these effects can be significantly enhanced (by factors $\sim 10^3 - 10^4$) in particular extensions of the SM. Searches for FCNC interactions have been carried out in $p\bar{p}$, e^+e^- and $e^\pm p$ collisions. At Tevatron, FCNC couplings can manifest themselves both in the form of anomalous single top quark production ($qg \rightarrow t$, $q = u, c$) or anomalous top quark decays ($t \rightarrow qV$, $q = u, c$ and $V = g, \gamma, Z$). Only the latter has been experimentally explored so far, via the search for $t \rightarrow q\gamma/Z$ decays.²⁵ The same $tq\gamma/Z$ interaction would be responsible for anomalous single top quark production in e^+e^- ($e^+e^- \rightarrow \gamma^*/Z \rightarrow tq$) and $e^\pm p$ ($eq \rightarrow et$) collisions, and searches have been performed at LEP²⁶ and HERA,^{27,28} respectively. Fig. 8 shows the existing 95% upper limits on the magnitude of the tuZ and $tu\gamma$ couplings.

Recently, H1 has reported²⁸ a 2.2σ excess in their search for single top quark production in the leptonic channels. A total of 5 events were observed, compared to 1.31 ± 0.22 events expected. No excess was observed in

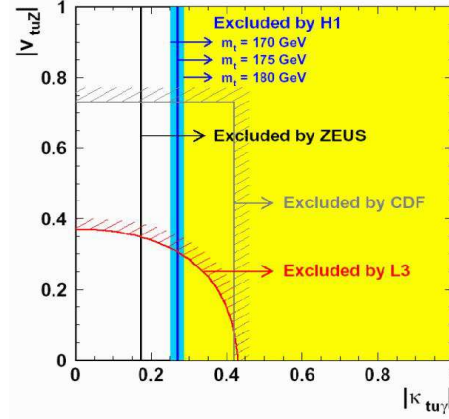


Figure 8. Exclusion limits at the 95% C.L. on the anomalous tuZ and $tu\gamma$ couplings obtained at the Tevatron, LEP (only L3 experiment shown) and HERA.

the hadronic channel. The combination of all channels yields a production cross section of $0.29^{+0.15}_{-0.14} \text{ pb}$. Interpreted as FCNC-mediated single top production, this measurement translates into $|\kappa_{tu\gamma}| = 0.20^{+0.05}_{-0.06}$. Higher statistics measurements at the Tevatron Run II and HERA-II should be able to confirm or exclude this measurement.

9 Searches for New Particles in Top Quark Production and Decay

Many models beyond the SM predict new particles preferentially coupled to the top quark: heavy vector gauge bosons (e.g. $q\bar{q} \rightarrow Z' \rightarrow t\bar{t}$ in Topcolor), charged scalars (e.g. $t \rightarrow H^+b$ in generic 2HDM), neutral scalars (e.g. $g\bar{g} \rightarrow \eta_T \rightarrow t\bar{t}$ in Technicolor) or exotic quarks (e.g. $q\bar{q} \rightarrow W^* \rightarrow t\bar{b}'$ in E_6 GUT). Because of the large spectrum of theoretical predictions, experimentally it is very important to develop searches as model-independent as possible. These analyses usually look for deviations in kinematic properties (e.g. $t\bar{t}$ invariant mass or top p_T spectrum), compare cross section measurements in different decay channels, etc.

In Run I, a model-independent search for a narrow heavy resonance X decaying to $t\bar{t}$ in the *lepton plus jets* channel was performed.²⁹ The obtained experimental upper limits on $\sigma_X \times B(X \rightarrow t\bar{t})$ vs M_X were used to exclude a leptophobic X boson³⁰ with $M_X < 560$ GeV (DØ) and $M_X < 480$ GeV (CDF) at 95% C.L.. Similar searches are underway in Run II.

In Run II, CDF has performed a search for $t \rightarrow H^+ b$ decays in $t\bar{t}$ events. If $M_{H^+} < m_t - m_b$, $t \rightarrow H^+ b$ competes with $t \rightarrow W^+ b$ and results in $B(t \rightarrow Wb) < 1$. Since H^\pm decays are different than W^\pm decays, $\sigma_{t\bar{t}}$ measurements in the various channels would be differently affected. By performing a simultaneous fit to the observation in the *dilepton*, *lepton plus tau* and *lepton plus jets* channels, CDF has determined model-dependent exclusion regions in the $(\tan\beta, M_H^\pm)$ plane.

10 New Physics Contamination in Top Quark Samples

Top quark events constitute one of the major backgrounds to non-SM processes with similar final state signature. As a result, top quark samples could possibly contain an admixture of exotic processes. A number of model-independent searches have been performed at the Tevatron in Run I and Run II.

A slight excess over prediction in the *dilepton* channel (in particular in the $e\mu$ final state) was observed in Run I.³¹ Furthermore, some of these events had anomalously large lepton p_T and \cancel{E}_T , which called into question their compatibility with SM $t\bar{t}$ production. In fact, it was suggested that these events would be more consistent with cascade decays from pair-produced heavy squarks.³² In Run II, CDF and DØ continue to scrutinize the *dilepton* sample. To date, the event kinematics appears to be consistent with SM $t\bar{t}$ production.^{33,9} Nevertheless, the flavor anomaly persists: the total number of events observed by both CDF and DØ in the

$e\mu(ee + \mu\mu)$ final state is 17(9), whereas the SM prediction is $10.2 \pm 1.0(9.4 \pm 1.0)$. More data is being analyzed and a definite conclusion on the consistency of the *dilepton* sample with the SM should be reached soon.

Also ongoing in Run II is the search for pair production of a heavy t' quark, with $t' \rightarrow Wq$. The final state signature would be identical to $t\bar{t}$, but the larger mass of the t' quark would cause the events to be more energetic than $t\bar{t}$. The current analysis is focused on the *lepton plus jets* channel and considers the H_T distribution as the observable to search for $t'\bar{t}'$ production. It is expected that with $L = 2 \text{ fb}^{-1}$, $m_{t'} < 300$ GeV will be excluded at the 95% C.L..

11 Conclusions

Till the beginning of the LHC, the Tevatron will remain the world's only top quark factory and a comprehensive program of top quark measurements is well underway. The excellent performances of the accelerator and the CDF and DØ detectors open a new era of precision measurements in top quark physics, required to unravel the true nature of the top quark and possibly shed light on the EWSB mechanism. This is a largely unexplored territory, and thus it has the potential to reveal signs of new physics preferentially coupled to the top quark. Most existing measurements appear to be in agreement with the SM, but there are a number of tantalizing (although not statistically significant) anomalies, which should definitely be clarified with the large data samples expected from the Tevatron till the end of 2009. Furthermore, techniques developed at the Tevatron to carry out this rich program of precision top quark physics will be an invaluable experience for the LHC.

Acknowledgments

The author would like to thank the conference organizers for their invitation and a

stimulating and enjoyable conference.

References

1. CDF Collaboration, F. Abe *et al.*, *Phys. Rev. Lett.* **74**, 2626 (1995); DØ Collaboration, S. Abachi *et al.*, *Phys. Rev. Lett.* **74**, 2632 (1995).
2. R. Bonciani, S. Catani, M.L. Mangano, and P. Nason, *Nucl. Phys. B* **529**, 424 (1998); N. Kidonakis and R. Vogt, *Phys. Rev. D* **68**, 114014 (2003); M. Cacciari *et al.*, *JHEP* **404**, 68 (2004).
3. N. Cabibbo, *Phys. Rev. Lett.* **10**, 531 (1963); M. Kobayashi and T. Maskawa, *Prog. Theor. Phys.* **49**, 652 (1973).
4. S. Eidelman *et al.*, *Phys. Lett. B* **592**, 1 (2004).
5. J.H. Kühn, *Acta Phys. Polon. B* **12**, 347 (1981); J.H. Kühn, *Act. Phys. Austr. Suppl.* XXIV, 203 (1982); I.Y. Bigi *et al.*, *Phys. Lett. B* **181**, 157 (1986).
6. CDF Collaboration, T. Affolder *et al.*, *Phys. Rev. D* **64**, 032002 (2001); DØ Collaboration, V.M. Abazov *et al.*, *Phys. Rev. D* **67**, 012004 (2003).
7. N. Kidonakis, *Phys. Rev. D* **64**, 014009 (2001); N. Kidonakis, E. Laenen, S. Moch, and R. Vogt, *Phys. Rev. D* **64**, 114001 (2001).
8. CDF Collaboration, D. Acosta *et al.*, *Phys. Rev. Lett.* **93**, 142001 (2004).
9. DØ Collaboration, V.M. Abazov *et al.*, *hep-ex/0505082*.
10. CDF Collaboration, D. Acosta *et al.*, *Phys. Rev. D* **71**, 052003 (2005).
11. DØ Collaboration, V.M. Abazov *et al.*, *hep-ex/0504058*.
12. CDF Collaboration, D. Acosta *et al.*, *Phys. Rev. D* **72**, 032002 (2005).
13. DØ Collaboration, V.M. Abazov *et al.*, *hep-ex/0504043*.
14. CDF Collaboration, DØ Collaboration and Tevatron Electroweak Working Group, *hep-ex/0404010*.
15. DØ Collaboration, V.M. Abazov *et al.*, *Nature* **429**, 638 (2004).
16. U. Baur, A. Juste, L.H. Orr, and D. Rainwater, *Phys. Rev. D* **71**, 054013 (2005).
17. B.W. Harris *et al.*, *Phys. Rev. D* **66**, 054024 (2002); Z. Sullivan, *Phys. Rev. D* **70**, 114012 (2004).
18. T. Tait and C.-P. Yuan, *Phys. Rev. D* **63**, 014018 (2001).
19. CDF Collaboration, D. Acosta *et al.*, *Phys. Rev. D* **71**, 012005 (2005).
20. DØ Collaboration, V.M. Abazov *et al.*, *Phys. Lett. B* **622**, 265 (2005).
21. DØ Collaboration, V.M. Abazov *et al.*, *Phys. Rev. D* **72**, 011104(R) (2005).
22. CDF Collaboration, D. Acosta *et al.*, *Phys. Rev. D* **71**, 031101 (2005); DØ Collaboration, V.M. Abazov *et al.*, *Phys. Lett. B* **617**, 1 (2005).
23. CDF Collaboration, T. Affolder *et al.*, *Phys. Rev. Lett.* **86**, 3233 (2001).
24. CDF Collaboration, D. Acosta *et al.*, *Phys. Rev. Lett.* **95**, 102003 (2005).
25. CDF Collaboration, F. Abe *et al.*, *Phys. Rev. Lett.* **80**, 2525 (1998).
26. Only the most sensitive result quoted: L3 Collaboration, P. Achard *et al.*, *Phys. Lett. B* **549**, 290 (2002).
27. ZEUS Collaboration, S. Chekanov *et al.*, *Phys. Lett. B* **559**, 153 (2003).
28. H1 Collaboration, A. Aktas *et al.*, *Eur. Phys. J. C* **33**, 9 (2004).
29. CDF Collaboration, T. Affolder *et al.*, *Phys. Rev. Lett.* **85**, 2062 (2000); DØ Collaboration, V.M. Abazov *et al.*, *Phys. Rev. Lett.* **92**, 221801 (2004).
30. R.M. Harris, C.T. Hill, and S.J. Parke, *hep-ph/9911288* (1999).
31. CDF Collaboration, F. Abe *et al.*, *Phys. Rev. Lett.* **80**, 2779 (1998); DØ Collaboration, S. Abachi *et al.*, *Phys. Rev. Lett.* **79**, 1203 (1997).
32. R.M. Barnett and L.J. Hall, *Phys. Rev. Lett.* **77**, 3506 (1996).
33. CDF Collaboration, D. Acosta *et al.*, *Phys. Rev. Lett.* **95**, 022001 (2005).